



ISSN NO. 2320-5407

Journal Homepage: - www.journalijar.com

INTERNATIONAL JOURNAL OF ADVANCED RESEARCH (IJAR)

Article DOI: 10.21474/IJAR01/17516
DOI URL: <http://dx.doi.org/10.21474/IJAR01/17516>



RESEARCH ARTICLE

REMOVAL OF PHENOL, A MUTAGENIC, SMALL-SIZED SUBSTANCE AND PRECURSOR OF MANY POLLUTANTS IN WATER

Saka Moussiliou¹, Elie Sogbochi¹, Cokou Pascal Agbangnan Dossa¹, Clément Kolawalé Balogoun¹, Guevara Nonviho^{1,2} and Dominique Codjo Koko Sohounhloue¹

1. Laboratory of Study and Research in Applied Chemistry, Polytechnic School of Abomey-Calavi, University of Abomey-Calavi (LERCA/EPAC/UAC), Benin.
2. Multidisciplinary Research Laboratory for Technical Education (LARPET), National University of Science, Technology, Engineering and Mathematics, Lokossa BP 133, Benin.

Manuscript Info

Manuscript History

Received: 10 July 2023

Final Accepted: 14 August 2023

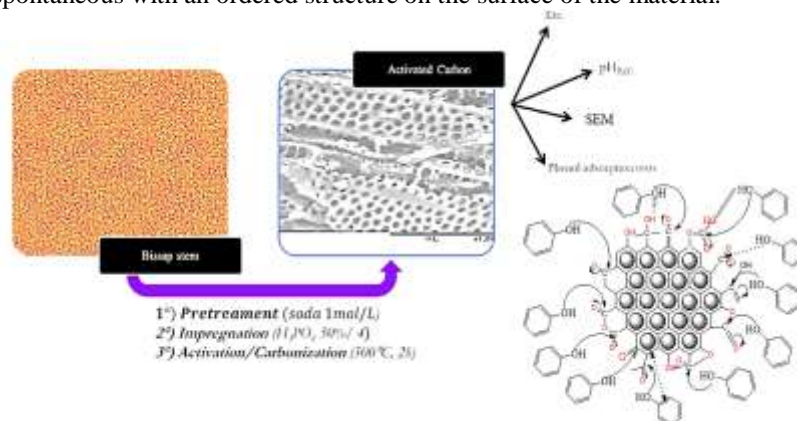
Published: September 2023

Key words:-

Waste, Pollution, Nosocomial Infections, Environment

Abstract

The present study aims at valorizing the stem of Hibiscus sabdariffa, a by-product of agriculture in Benin. This natural resource, abundant in tropical countries, including Benin, was until now considered as a biodegradable waste and treated as such. However, it possesses adsorption properties that can be exploited through its transformation into activated carbon for various uses, including water pollution control. For this purpose, activated carbon has been developed from Hibiscus sabdariffa stems chemically impregnated with phosphoric acid. The pseudo second-order model predicts the kinetics of phenol adsorption on the activated carbon produced. The thermodynamic study of the adsorption process of phenol shows that it is exothermic and spontaneous with an ordered structure on the surface of the material.



Copy Right, IJAR, 2023.. All rights reserved.

Introduction:-

Hibiscus sabdariffa is of the Malvaceae family, native to India and Malaysia [1,2]. This plant, known for its nutritional benefits, is often used by traditional therapists and by modern therapeutics because it is rich in phytochemicals like polyphenols [3]. During its operations, it generates large quantities of by-products such as hulls,

Corresponding Author:- Cokou Pascal Agbangnan Dossa

Address:- Laboratory of Study and Research in Applied Chemistry, Polytechnic School of Abomey-Calavi, University of Abomey-Calavi (LERCA/EPAC/UAC), Benin.

stems, leaves, These biodegradable wastes are left in the fields or burned to make room for other crops. The lignocellulosic residues generated by Hibiscus sabdariffa deserve a valorization like the other woody coproducts. Its by-products can be valorised by chemical and energetic ways.

The transformation of these lignocellulosic wastes into activated carbon allows to eliminate them in a rational way with more respectful methods to the environment. But also, the activated carbon is a useful material in several fields notably in the sector of water treatment.

Phenol (an azo compound) is a reference molecule used to evaluate the capacity of adsorbents to remove molecules capable of adsorbing in ultramicropores and is also often found in industrial effluents. It is therefore necessary to remove them from the wastewater before discharge. It can be reduced to carcinogenic by-products in anaerobic products. Due to their high toxicity, phenolic compounds are particularly targeted in water pollution. Several methods are proposed to remove phenol and its derivatives. For this purpose, many treatment methods, such as chemical, physicochemical, and biological processes are used. Aerobic and anaerobic biodegradation, ozonation and removal by ion exchange resins are just some of the processes used [4]. Adsorption of phenol molecules by activated carbon is a highly effective technique that is widely used [5]. Among these methods, adsorption is very effective for the removal of organic and inorganic pollutants [6]. Activated carbon adsorption is a very popular method because of its very high external and internal surface area, its well-developed porous structure, and its favourable surface chemistry. Thus, we have produced activated carbon from the stems of Hibiscus sabdariffa by with phosphoric acid activation. This step was preceded a demineralization of the biomass with a molar solution of sodium hydroxide.

Materials And Method:-

Materials:-

The stems of Hibiscus sabdariffa variety sabdariffa were collected in the Valley farm in Bopa in the South - West of Benin; they are shelled, crushed, and sifted on a 2mm mesh screen and kept dry at the laboratory for testing. NaOH (Merck) was used to remove mineral matter from the stem. H₃PO₄ (Merck) was used as an activating agent. Hydrochloric acid (Merck) and distilled water to wash the activated carbons and phenol (Merck) is used as an adsorbate to investigate the adsorption efficiency of activated carbons.

Activated carbon from Hibiscus sabdariffa stems production.

The ground rods were washed with tap water, rinsed with distilled water, and dried at 110°C for 24 hours [7,8]. They were then washed with sufficient molar soda solution and dried at 110°C. After this initial drying, the pre-treated grindings were washed with tap water and rinsed with distilled water, then dried again at 110°C for 24 hours. The grindings were impregnated with phosphoric acid with an impregnation ratio (Xp): 4

$$X_p = \frac{m_{H_3PO_4}}{m_{Precursor}} \quad (1)$$

The carbonization was done at 500°C, programmed according to a gradient of 10°C.min⁻¹. After a stay of 2 hours at 500°C, the pyrolyzat was cooled inside the furnace before being removed. The pyrolyzat was thoroughly washed with a decimolar solution of hydrochloric acid and distilled water.

Thus, the activated carbons obtained were designated CA - THS₄ (activated carbon produced from Hibiscus sabdariffa stems of ratio 4).

Activated carbon was produced according to the scheme in Fig.1.

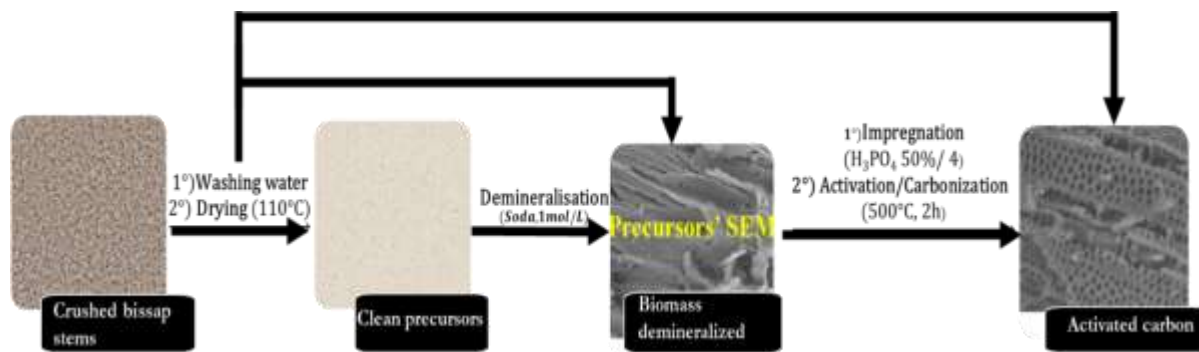


Figure 1:- The diagram of the elaboration of activated carbon from Hibiscus sabdariffa stems.

Characterization of the activated carbons

Scanning Electron Microscopy (SEM) observations of AC were performed using a HITACHI TM 3000 model with field effects that allow magnification. Before observation at the SEM, the samples were metallized using a Quorum model SC 620 metallizer by depositing a layer of palladium-gold (a few nanometers thick) to make the materials more conductive.

The zero charge point pH (pHpzc) was determined for activated carbons using the pH derivative method developed by Lopez-Ramon et al. [9].

Study of the adsorption of phenol on the activated carbons from Hibiscus sabdariffa stems

Study of kinetics and effect of initial concentration

The adsorption kinetics are studied in order to determine the quantity of phenol adsorbed at different time intervals and the equilibrium time. A mass m of activated carbon was suspended in a solution of volume V and initial concentration C_0 . Samples were taken at predetermined time intervals and separated using a syringe equipped with filters (0,45 μ m). The analysis of the residual concentration of the adsorbate (Fig. 2) was performed by UV-Visible absorption spectrophotometry at $\lambda = 270$ nm, where the dye solution absorbs lighter. The results obtained are plotted in the form of curves $q_t = f(t)$ and $R(\%) = f(t)$. The amount of adsorbed dye q_t (mg/g) and the removal rate R (%) are calculated as follows [5,10]:

$$q_t = \frac{(C_0 - C) \times V}{m} \quad (2)$$

$$R(\%) = \frac{C_0 - C}{C_0} \times 100 \quad (3)$$

where C_0 and C are the initial and at time t (min) of adsorbates concentration (mg.L⁻¹), V the volume of solution (L) and m the dry weight of the added adsorbent (g).

Figure 2:- Chemical formula of phenol.

Different models used for adsorption kinetics and isotherm

Table 1 summarises the various models used to study the kinetics and model of adsorption isotherms. The linear and non-linear forms of these models used are given in the table.

Table 1:- Adsorption kinetics and isotherm models [7,8,11–13].

Models	Non-linear form	Linear form	Parameters
Models of adsorption kinetics			
Pseudo-first order	$q_t = q_e(1 - e^{-k_1 t})$	$\ln(q_e - q_t) = \ln q_e - k_1 t$	K_1 is the kinetic constant of the adsorption reaction (min^{-1})
Pseudo-second order	$q_t = \frac{k_2 q_e^2 t}{1 + k_2 q_e t}$	$\frac{t}{q_t} = \frac{1}{k_2 q_e^2} + \frac{t}{q_e}$	K_2 is the second-order reaction rate constant for adsorption ($\text{g.mg}^{-1}.\text{min}^{-1}$).
Weber and Morris	$q_t = k_i t^{1/2} + c$	-	K_1 is the intraparticle diffusion constant and C is the intersection of the straight line with the y-axis or the intercept at the origin.
Elovich	-	$q_t = \frac{1}{\beta} \ln(\alpha\beta) + \frac{1}{\beta} \ln(t)$	α is the initial adsorption rate (mg/g.min); $t_0 = 1/(\alpha.\beta)$ and β : constant linked to the external surface and the chemisorption activation energy (g.mg^{-1}).
Adsorption isotherm models			
Langmuir	$q_e = \frac{q_m k_L C_e}{1 + k_L C_e}$	$\frac{C_e}{q_e} = \frac{1}{q_m k_L} + \frac{C_e}{q_m}$	q_{\max} represents the maximum adsorption capacity of the solid phase charge (mg.g^{-1}) and K_L : Langmuir coefficient.
Freundlich	$q_e = K_F C_e^{1/n}$	$\ln q_e = \ln K_F + \frac{1}{n} \ln C_e$	K_F and n sont les constantes de Freundlich liées à la capacité d'adsorption et à l'intensité d'adsorption respectivement.
Tempkin	$C_e = \frac{1}{A} \exp\left(\frac{q_e}{B}\right)$	$q_e = B \ln A + B \ln C_e$	A is the Tempkin equilibrium binding constant (L.mg^{-1}) corresponding to the maximum binding energy, B is the constant related to the heat of adsorption, T is the absolute temperature and R is the universal constant of perfect gases.

Influence of temperature on phenol adsorption

To study the effect of temperature on the adsorption of phenol, we introduced in several Erlenmeyer flasks 0.1g of activated carbon and 100mL of the phenol solution. The mixture was shaken by varying the temperature at 20, 40 and 50°C. Following equations were used to calculate the thermodynamic parameters, such as: free energy ΔG° , enthalpy ΔH° and entropy ΔS° [14,15]:

$$\Delta G^\circ = \Delta H^\circ - T\Delta S^\circ \quad (4)$$

$$\ln\left(\frac{q_e}{C_e}\right) = \frac{\Delta S^\circ}{R} - \frac{\Delta H^\circ}{RT} \quad (5)$$

Results And Discussion:-

Surface analysis by Scanning Electron Microscope (SEM)

Fig. 3. shows SEM micrographs of activated carbon at different magnifications. SEM images of the activated carbon show that the thick wall opens up and a wider porosity is created, thus the outer surfaces of the chemically activated carbon are full of cavities [15].

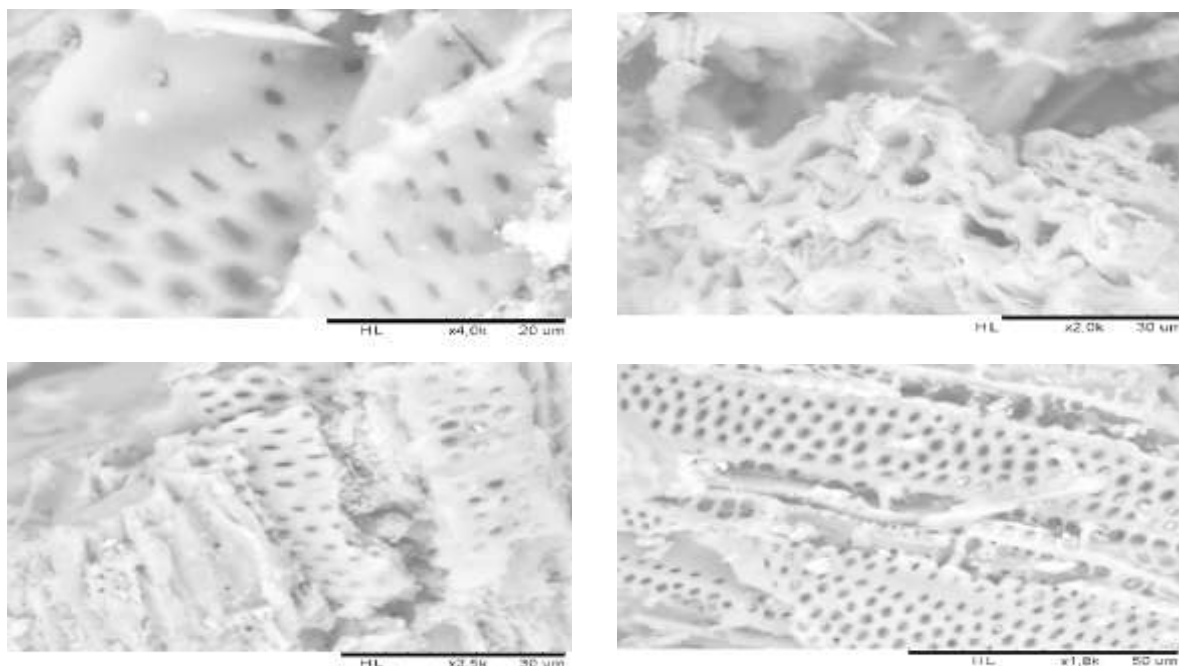


Figure 3:- Scanning electron micrographs their activated carbon of Hibiscus sabdariffa stems.

Textural properties of activated carbons from Hibiscus sabdariffa stems

Table 2 shows the textural properties of the activated carbon investigated in this study. We carried out a comparative calculation of the specific surface areas using two models: the BET model corrected by Rouquerol and the 2D-NLDFT model. We note that the specific surface area obtained from the model is slightly higher than that obtained from the 2D-NLDFT model (BET: $1053 \text{ m}^2 \cdot \text{g}^{-1}$ versus 2D-NLDFT: $975 \text{ m}^2 \cdot \text{g}^{-1}$). Secondly, the microporous volume is higher than the mesoporous volume. This results in a higher rate of micropores. Consequently, the surface area determined by the BET model is increased because, by hypothesis, it is more useful for characterising mesoporous materials. The carbonaceous material is therefore more suitable for trapping small molecules.

Table 2:- Textural properties of the activated carbons from Hibiscus sabdariffa stems.

Activated carbons	Xp	S ($\text{m}^2 \cdot \text{g}^{-1}$)		V_{μ} ($\text{m}^3 \cdot \text{g}^{-1}$)	V_{μ} (%)	V_{meso} ($\text{m}^3 \cdot \text{g}^{-1}$)	V_{meso} (%)	V_T ($\text{m}^3 \cdot \text{g}^{-1}$)
		BET	2D-NLDFT					
CA – THS ₄	4:1	1053	975	0.39	56%	0.31	44%	0.70

pH at zero load point (pHpzc) of activated carbon

The pHpzc indicates the acid-base character of the surface functions of the porous materials. It is also the point at which the charge of the positive surface sites is equal to that of the negative surface sites [16]. Fig. 4 shows the pHpzc determination curve for the activated carbon studied. For this carbon, the pHpzc ≈ 2.8 lower than 7. This value reveals the acidic character of the surface chemical functions of the activated carbon [17].

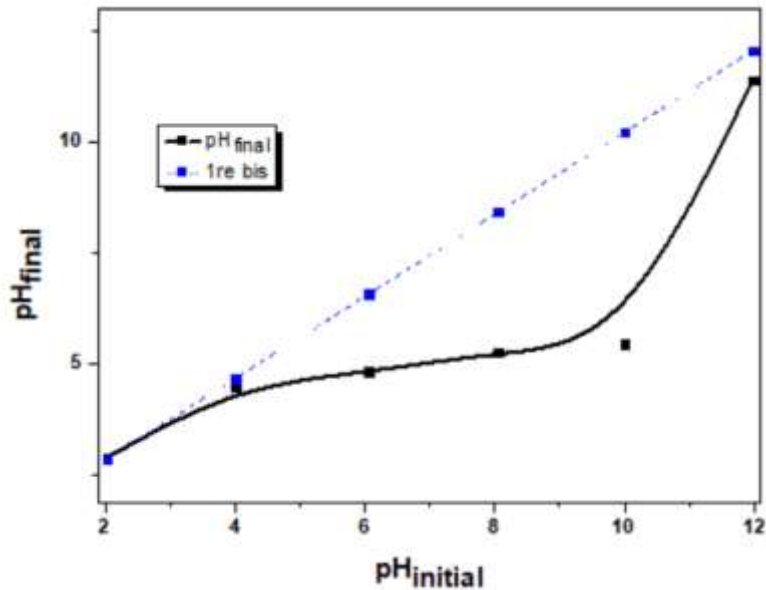


Figure 4:- pH_{zpc} determination curve.

Adsorption tests of phenol on activated carbon from *Hibiscus sabdariffa* stems.

Study of phenol adsorption kinetics on activated carbon from *Hibiscus sabdariffa* stems

The experimental results indicate a rapid increase in adsorption capacity during the first five (05) minutes; this indicates that the adsorption rate is also very high; but the equilibrium times no longer depend on the initial concentration. The equilibrium is reached after 5 min. It appears from the results obtained that the elimination rate of phenol is low, less than 65% whatever the initial concentration. We can also note that the quantity of adsorbates adsorbed increases according to the initial concentration (Fig. 5 and 6).

The rapidity of reaction during the first minutes explains that the number of active sites available on the surface of the activated carbon is much greater than that of the sites remaining after a certain time. For the rest of the not adsorbed quantity is interpreted by the saturation of the surface of the activated carbon.

Studies on phenol adsorption revealed that electron donor-receptor interaction, electron dispersive coupling interaction and competition for adsorption of water molecules [6]. Water also influences the adsorption of phenol on activated carbon. This occurs when some of the more active sites that adsorb phenol molecules are blocked by the adsorption of water molecules. The carboxyl and hydroxyl groups inhibit the adsorption of phenol and increase the affinity of the carbon with water.

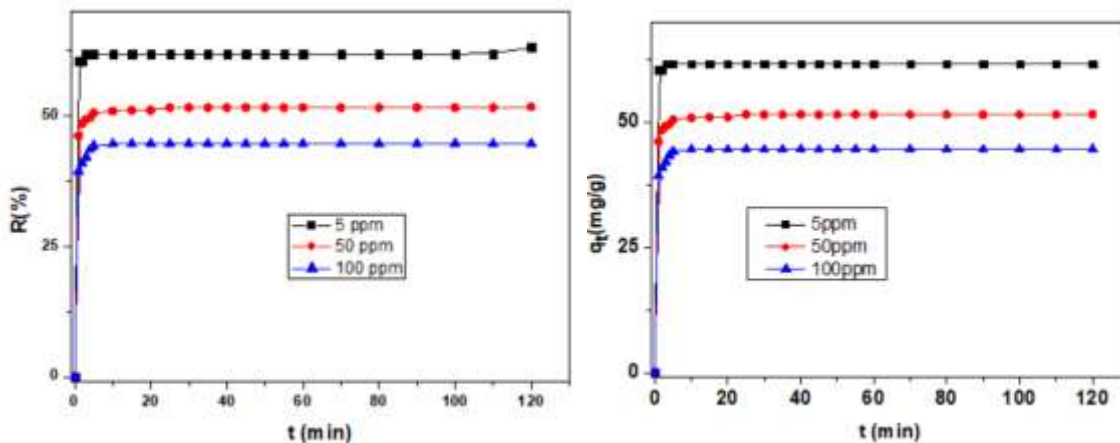


Figure 5:- Study of phenol adsorption kinetics on activated carbon.

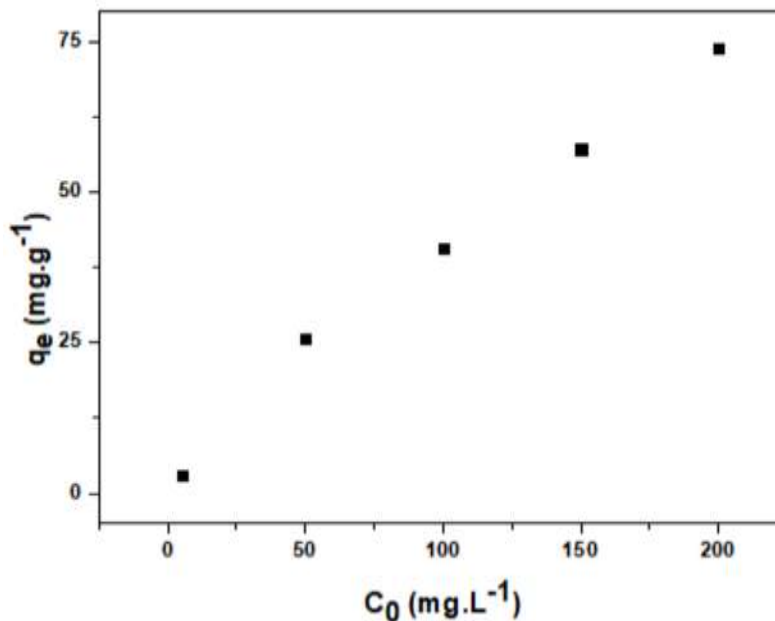


Figure 6:- Effect of the initial concentration on the adsorption capacity of activated carbon.

Mechanism of the phenol adsorption reaction on bissap stem activated carbon

Fig.7 explains the phenol adsorption mechanism on the activated carbon surface. Sogbochi et al. (2022) have shown in this figure that activated carbons from the shell of *Lophira Lanceolata* prepared thermochemically with orthophosphoric acid fix phenol molecules by means of various interactions. The adsorption mechanism involves electrostatic interactions and fixation by the formation of covalent bonds.

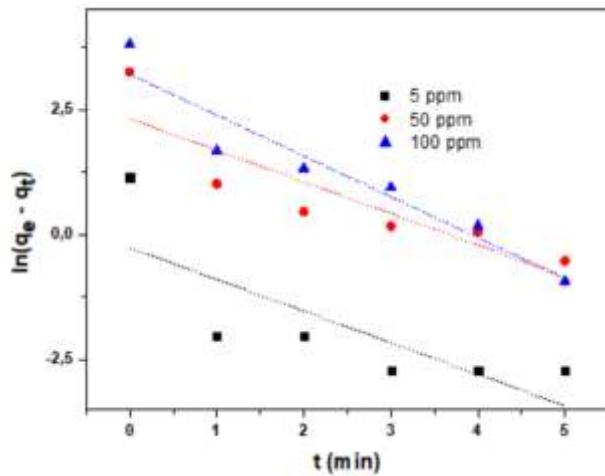
Figure 7:- Mechanism of liaisons formation between the adsorbate and the surface functions of the activated carbon [7].

Modelling of phenol adsorption kinetics on activated carbon from Hibiscus sabdariffa stems

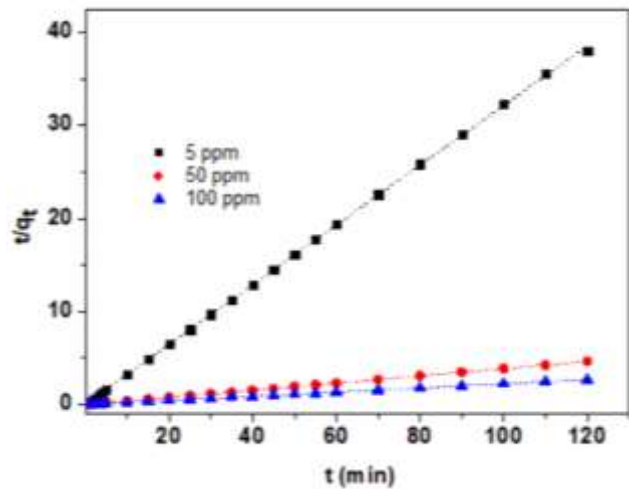
The adsorption kinetics of phenol on activated carbon was studied for initial concentrations 5, 50 and 100 ppm of phenol in aqueous solution.

The values of the kinetic parameters of the phenol adsorption reaction were calculated (Table 3) from the slopes and intercepts underlying the linearized forms of each model. The higher the correlation factor, the better the model for studying the adsorption process. From the results in Table 1, we note that the pseudo second order model has the highest correlation coefficients, so we can deduce that it is the model that best describes the adsorption process of phenol on activated carbon. Furthermore, the correlation of this model with the experimental data is characterized by the values of $q_{e,cal}$ very close to the values of $q_{e,exp}$. This indicates that the adsorption process of phenol could be controlled by chemisorption which involves valence forces through the sharing or exchange of electrons between the adsorbent and the adsorbate. The study of phenol adsorption kinetics by other researchers has also shown that the pseudo-second order rate is the one that simulates phenol adsorption with good agreement.

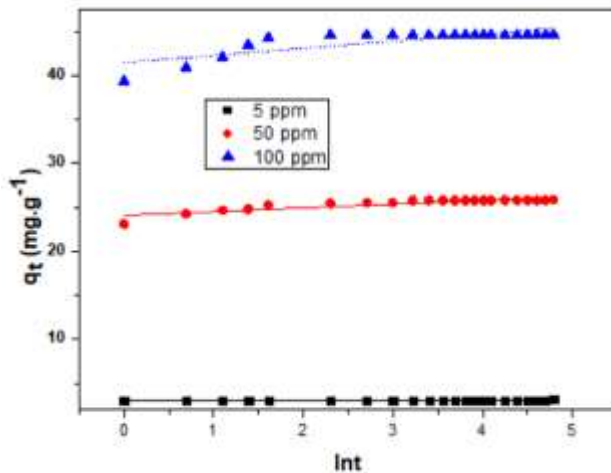
The intraparticle diffusion is not the determining step of the adsorption process because the corresponding lines do not pass through the origin of the reaction (C is not zero). C not being zero, confirms that the curve $qt = f(t^{1/2})$ has more than one linear portion (Figure 10)[6]. The curves are not linear over the entire time range, showing that more than one process affects the adsorption of phenol. From Figure 10, there are two different steps, the plot shows bilinearity indicating the existence of several steps. Thus, the first slightly concave stage, characterizes the phenomenon of diffusion on the external surface of the activated carbon, it is the instantaneous adsorption, the second linear part, corresponds to the stage where the adsorption could be controlled by the phenomenon of intraparticle diffusion [18].



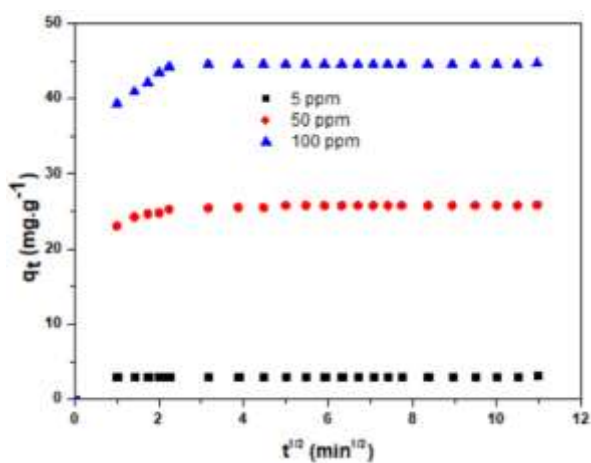
(a) Pseudo-first order kinetic model



(b) Pseudo-second order kinetic model



(c) Elovich kinetic model



(d) Intraparticle diffusion model

Figure 8:- Kinetic curves of phenol adsorption by activated carbon derived from Hibiscus sabdariffa stems.

	C_0 (mg.L ⁻¹)	5	50	100
	$q_{e,exp}$ (mg.g ⁻¹)	3.09	25.79	44.61
Pseudo-First Order	$q_{e,cal}$ (mg.g ⁻¹)	0.77	10.11	24.55
	K_1 (min ⁻¹)	0.63	0.63	0.82
	r^2_1	0.521	0.731	0.899
Pseudo-second ordre	$q_{e,cal}$ (mg.g ⁻¹)	3.11	25.85	44.66
	K_2 (min ⁻¹)	1.79	0.29	0.28
	r^2_2	0.999	1.000	1.000
Elovich Model	α	$1.39.10^{13}$	$9.21.10^{23}$	$1.37.10^{22}$
	β	86.81	2.33	1.23
	R^2	0.40178	0.77377	0.63918
Intraparticle diffusion	k_i	0.08	0.74	1.29
	C	2.52	20.15	34.82
	R^2	0.11537	0.16995	0.17173

Table 3:- Kinetic model constants for phenol adsorption.

Table 4 summarises the parameters of the kinetic models that best fit the phenol adsorption process on various adsorbent materials. The pseudo-second order kinetic model is largely the model that best represents the experimental results of phenol adsorption, which is consistent with the work of this thesis, and the other kinetic models are very rare. The resulting pseudo-second order model and its parameters agree with the results of the present study. For, the temperature range used is [25; 30], the coefficients of determination are very close to unity and the rate constant k_2 is very small.

The pseudo-first-order model obtained by Yan et al. (2020) would indicate that this group of researchers considered the very first minutes of the phenomenon when equilibrium was not reached in their work. This latter aspect is verified in the case of their work, given the kinetic curves represented from experimental points not having an asymptote of reaction equilibrium, as shown in Fig. 9.

Table 4:- Summary of the parameters of the models best suited for modelling the kinetics of phenol adsorption on various adsorbent materials.

Adsorbent	Model	T (°C)	K_2 (g.min.mg ⁻¹)	r^2_2	Reference
Coconut activated carbon	Pso	-	0.005606	0.9981	[19]
Hematite iron oxide nanoparticles (α -Fe ₂ O ₃)	Pso	-	0.019	0.993	[20]
Palm oil shell biosorbent	Pso	-	0.00144	0.992	[13]
Double-layer hydroxide Zn-Al	Pso	25	0.0119	0.9998	[21]
Activated carbon from rice husk	Pso		0.01	0.9994	[22]
Clay	Pso	30	0.008	0.98	[23]
Activated carbon from Tithonia diversifolia	Pso	25	0.04	0.99	[24]
Activated carbon from Kraft lignin	Pso	25	0.00028	1.00	[18]
Commercial activated carbon	Pso	25	0.18	0.999	[25]
Activated carbon pellet	Pfo	30	$K_1 = 0.0103$	0.9134	[26]
Pfo : Pseudo-first order; Pso : Pseudo-second order					

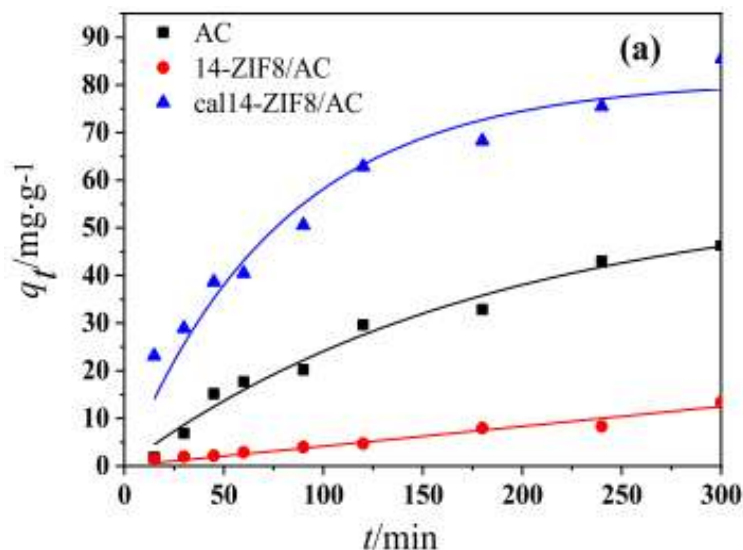


Figure 9:- Phenol adsorption kinetics curves for work carried out by Yan et al. (2020).

Adsorption isotherms of phenol

Table 5 shows the isothermal parameters and correlation coefficient estimated by these isothermal models for phenol adsorption. The correlation coefficient value of the Freundlich model is higher than that of the Langmuir ($R^2_L = 0.8721$) and Tempkin models. From this observation, it appears that the Freundlich model is the most credible to explain the adsorption of phenol on activated carbon. The Freundlich adsorption isotherm assumes that adsorption occurs on a heterogeneous surface by a multilayer adsorption mechanism, and that the amount adsorbed increases with concentration (Fig. 10) [27]. The adsorption capacity of the calculated from the Langmuir adsorption model for is 113 mg/g and is even better compared to the results encountered in the literature. This can be explained by the high microporosity of the coal, i.e., 56% of the micropore rate. The separation factor obtained from equation (4) in the range 0-1, indicating that the removal of phenol is favourable for adsorption. The value of adsorption intensity (n) is greater than one shows that activated carbon made from bissap stems is an excellent adsorbent for the removal of phenolic compounds. The constant A of the Tempkin isotherm 0.44 L.mg^{-1} and the constant B of the isotherm for the heat of adsorption of phenol on activated carbon were estimated to be 15.17 J.mol^{-1} , indicating that electrostatic interaction and pore heterogeneity play an important role in the adsorption since it is greater than 1.

The adsorption capacity of phenol is influenced by the surface chemistry, probably due to the presence of surface functional groups and heteroatoms of the activated carbon. Xiong et al. (2020) showed that phenol was removed more efficiently at alkaline pH, however, pH affects the ionic state of the surface functional groups [28,29]. In this study, the effect of pH was not determined, however, the pH_{pzc} indicates the acidic nature of the activated carbon which decreases its affinity to phenol which has a labile hydrogen of the -OH group giving it an acidic character; therefore, better removal of phenol can be projected on the developed activated carbon.

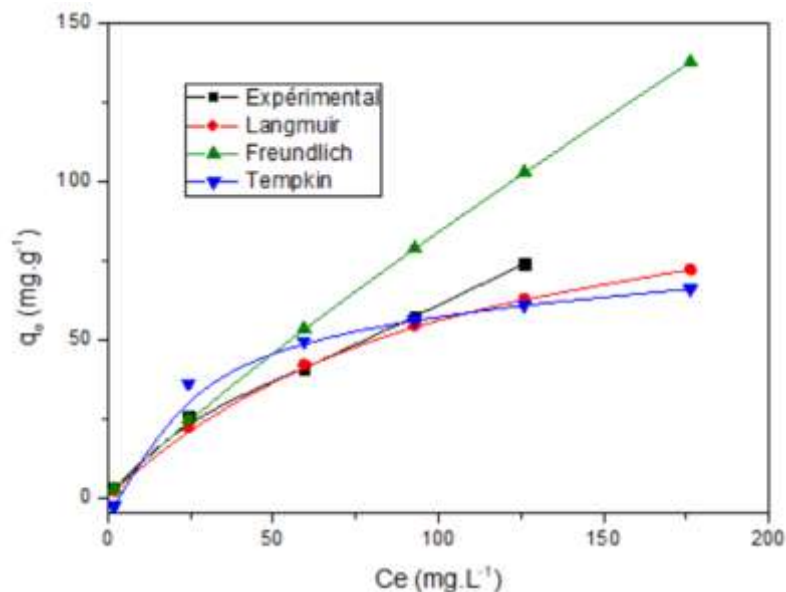


Figure 10:- Adsorption isotherms of phenol on the activated carbon from Hibiscus sabdariffa stems.

Table 5:- Isothermal parameters and correlation coefficient estimated by these isothermal models for phenol adsorption

Langmuir Isotherm	q_m ($\text{mg}\cdot\text{g}^{-1}$)	113
	K_L ($\text{L}\cdot\text{mg}^{-1}$)	0.01
	R_L^2	0.87261
Freundlich Isotherm	$1/n$	0.87
	k_F ($(\text{mg}\cdot\text{g}^{-1})(\text{L}\cdot\text{g}^{-1})^{1/n}$)	1.53
	R_F^2	0.88868
Tempkin Isotherm	A ($\text{L}\cdot\text{g}^{-1}$)	0.44
	B	15.17
	R_T^2	0.82761

Table 6 shows the parameters of the mathematical approaches that best fit the adsorption process of phenol on various adsorbent materials. These studies are carried out at temperatures between 25 and 55 °C, to give adsorption capacities that range from 6 to 246 $\text{mg}\cdot\text{g}^{-1}$, when the initial concentration reaches 500 $\text{mg}\cdot\text{L}^{-1}$. It is particularly interesting to note that the maximum adsorption capacities obtained in this study are higher than those reported in the literature. The very large specific surface and a developed microporosity could be at the origin of this high adsorption capacity. The high initial concentration (1500 $\text{mg}\cdot\text{L}^{-1}$) observed could also justify this behaviour.

It should be noted that the Langmuir approach is not as widely used as a model that best describes the phenol adsorption process, however it is often used to determine the binding capacity of phenol molecules. These values should be taken with care, especially as they are derived from the model with a low coefficient of determination.

The adsorption of phenol in most cases, as in this study, followed the Freundlich model and afterwards the Langmuir model and only a few took place via different models such as Redlich-Peterson and Brouers-Sotolongo.

Table 6:- Summary of parameters for the modelling of phenol adsorption isotherms for various adsorbent materials.

Adsorbent	T (°C)	C_0 ($\text{mg}\cdot\text{L}^{-1}$)	Model	q_{max} ($\text{mg}\cdot\text{g}^{-1}$)	Reference
Activated carbon from rice bran	27	-	Langmuir	6.16	[30]
Active carbon from vetiver roots	25	20 - 100	Brouers-Sotolongo and Redlich-Peterson	21.69	[31]

Activated carbon from black acacia bark waste	55	50 - 500	Freundlich	98.57	[32]
Activated charcoal from tobacco residues	-	1 - 12	Langmuir	17.83	[15]
Activated carbon from soya straw	-	10 - 500	Freundlich	278.0	[33]
Single-walled carbon nanotubes	30	25 - 350	Freundlich	549.60	[34]
Biochar from oil palm fronds	25	40 - 260	Freundlich	57.48	[5]
Activated carbon from Tithonia diversifolia		100 - 500	Langmuir	50.552	[24]
Lignite activated carbon	25	-	Freundlich	42.3191	[35]
Bioadsorbent the neem (Azadirachta indica)	-	100 - 500	Freundlich	74.90636	[36]
Commercial activated carbon	-	10 - 400	Langmuir	246.31	[37]

Effect of temperature on the adsorption capacity of phenol by activated carbon

The results of the thermodynamic parameters deduced from Fig.11 are shown in Table 7. From these results, it is observed that the free energy is positive in all cases. This indicates that the adsorption of phenol on activated carbon is not spontaneous whatever the temperature, the adsorption process of phenol on activated carbon is chemisorbed since the values of $\Delta H^\circ > 40 \text{ kJ.mol}^{-1}$ [8,15]. The free enthalpy is negative, which implies that the adsorption process is exothermic, This indicates the decrease in the adsorption capacity value of the adsorbent with increasing temperature [15]. ΔS° is negative, which means that the phenol molecules remain more and more ordered on the solid/solution interface during the adsorption process [15].

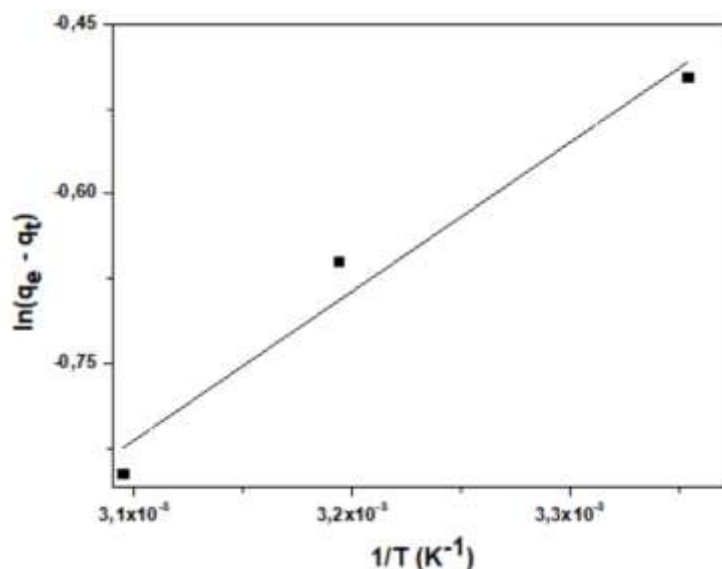


Figure 10:- Effect of temperature on the adsorption capacity of phenol by activated carbon.

Table 7:- Thermodynamic parameters ΔG° , ΔH° and ΔS° related to the adsorption of phenol on activated carbon. CA – THS4.

Sample	C_0 (mg.L ⁻¹)	T (K)	ΔG° : (kJ.mol ⁻¹)	ΔH° (kJ.mol ⁻¹)	ΔS° (kJ.mol ⁻¹ .K ⁻¹)
CA – THS ₄	100	293.15	-3212854	41	11
		313.15	-3432052		
		323.15	-3541651		

Conclusion:-

During this study, we explored the possibility of valorization of bissap stems to remove phenolic compounds from wastewater. For this purpose, we elaborated activated carbon by activation with phosphoric acid. The pH_{pzc}, phenol adsorption tests and comparison of adsorption results to literature values are done.

The pH_{pzc} reveals the acidic nature of the activated carbon and the high rate of micropores is confirmed by good binding of phenol molecules. The pseudo-second order model is the most appropriate to represent the kinetic behaviour of phenol adsorption on activated carbon. The Freundlich model showed the best fit to the equilibrium data, indicating that the adsorption of phenol molecules in water provided the knowledge that this species adsorbs through the superposition of several layers (multilayer).

Declaration of Competing Interest

The authors declare that they have no known competing financial interests or personal relationships that could have appeared to influence the work reported in this paper.

Acknowledgement:-

This work received no funding. No funding is available for open access publications from our institution or other sources

References:-

1. F.J. Alarcon-Aguilar, A. Zamilpa, M.D. Perez-Garcia, J.C. Almanza-Perez, E. Romero-Nuñez, E.A. Campos-Sepulveda, L.I. Vazquez-Carrillo, R. Roman-Ramos, Effect of Hibiscus sabdariffa on obesity in MSG mice, *J. Ethnopharmacol.* 114 (2007) 66–71. <https://doi.org/10.1016/j.jep.2007.07.020>.
2. G. Riaz, R. Chopra, *Biomedicine & Pharmacotherapy* A review on phytochemistry and therapeutic uses of Hibiscus sabdariffa L., *Biomed. Pharmacother.* 102 (2018) 575–586. <https://doi.org/10.1016/j.biopha.2018.03.023>.
3. I. Jabeur, E. Pereira, L. Barros, R.C. Calhelha, M. Soković, M.B.P.P. Oliveira, I.C.F.R. Ferreira, Hibiscus sabdariffa L. as a source of nutrients, bioactive compounds and colouring agents, *Food Res. Int.* 100 (2017) 717–723. <https://doi.org/10.1016/j.foodres.2017.07.073>.
4. A. Dąbrowski, P. Podkościelny, Z. Hubicki, M. Barczak, Adsorption of phenolic compounds by activated carbon - A critical review, *Chemosphere.* 58 (2005) 1049–1070. <https://doi.org/10.1016/j.chemosphere.2004.09.067>.
5. A.A. Lawal, M.A. Hassan, M.A. Ahmad Farid, T.A. Tengku Yasim-Anuar, M.H. Samsudin, M.Z. Mohd Yusoff, M.R. Zakaria, M.N. Mokhtar, Y. Shirai, Adsorption mechanism and effectiveness of phenol and tannic acid removal by biochar produced from oil palm frond using steam pyrolysis, *Environ. Pollut.* 269 (2021). <https://doi.org/10.1016/j.envpol.2020.116197>.
6. A. Kumar, H.M. Jena, Removal of methylene blue and phenol onto prepared activated carbon from Fox nutshell by chemical activation in batch and fixed-bed column, *J. Clean. Prod.* 137 (2016) 1246–1259. <https://doi.org/10.1016/j.jclepro.2016.07.177>.
7. E. Sogbochi, G. Nonviho, P. Girods, S. Fontana, Removal of hydroxybenzene for the purpose of treating wastewater from the plastics industry using activated carbon obtained from Lophira lanceolata hulls., *J. Chem., Biol. Phys. Sci.* 13 (2023). <https://doi.org/10.24214/jcbps.D.13.1.05163>.
8. E. Sogbochi, P. Girods, G. Nonviho, S. Fontana, Y. Rogaume, D. Codjo, K. Sohounhloue, Use of Carbonaceous Materials Derived from Co-products of Lophira lanceolata for Adsorption Tests of Congo Red Dye, *Am. J. Phys. Chem.* 11 (2022) 91–101. <https://doi.org/10.11648/j.ajpc.20221104.12>.
9. M. V Lopez-ramon, F. Stoeckli, C. Moreno-castilla, F. Carrasco-marin, On the characterization of acidic and basic surface sites on carbons by various techniques, (1999) 1215–1221.
10. M.T. Nakhjiri, G. Bagheri Marandi, M. Kurdtabar, Preparation of magnetic double network nanocomposite hydrogel for adsorption of phenol and p-nitrophenol from aqueous solution, *J. Environ. Chem. Eng.* 9 (2021) 105039. <https://doi.org/10.1016/j.jece.2021.105039>.
11. J. Ouyang, L. Zhou, Z. Liu, J.Y.Y. Heng, W. Chen, Biomass-derived activated carbons for the removal of pharmaceutical micropollutants from wastewater: A review, *Sep. Purif. Technol.* 253 (2020) 117536. <https://doi.org/10.1016/j.seppur.2020.117536>.
12. M.A. Al-Ghouti, D.A. Da'ana, Guidelines for the use and interpretation of adsorption isotherm models: A review, *J. Hazard. Mater.* 393 (2020) 122383. <https://doi.org/10.1016/j.jhazmat.2020.122383>.

13. J.N. Sahu, R.R. Karri, N.S. Jayakumar, Improvement in phenol adsorption capacity on eco-friendly biosorbent derived from waste Palm-oil shells using optimized parametric modelling of isotherms and kinetics by differential evolution, *Ind. Crops Prod.* 164 (2021) 113333. <https://doi.org/10.1016/j.indcrop.2021.113333>.
14. T. Calvete, E.C. Lima, N.F. Cardoso, J.C.P. Vaghetti, S.L.P. Dias, F.A. Pavan, Application of carbon adsorbents prepared from Brazilian-pine fruit shell for the removal of reactive orange 16 from aqueous solution: Kinetic, equilibrium, and thermodynamic studies, *J. Environ. Manage.* 91 (2010) 1695–1706. <https://doi.org/10.1016/j.jenvman.2010.03.013>.
15. M. Kilic, E. Apaydin-Varol, A.E. Pütün, Adsorptive removal of phenol from aqueous solutions on activated carbon prepared from tobacco residues: Equilibrium, kinetics and thermodynamics, *J. Hazard. Mater.* 189 (2011) 397–403. <https://doi.org/10.1016/j.jhazmat.2011.02.051>.
16. M.T.I. A. Martínez de Yuso, B. Rubiob, Influence of activation atmosphere used in the chemical activation of almond shell on the characteristics and adsorption performance of activated carbons. *Fuel Processing Technology*, 119, 74–80., *Process. Technol.* 119 (2014) 74–80.
17. S. Das, S. Mishra, Insight into the isotherm modelling, kinetic and thermodynamic exploration of iron adsorption from aqueous media by activated carbon developed from Limonia acidissima shell, *Mater. Chem. Phys.* 245 (2020) 122751. <https://doi.org/10.1016/j.matchemphys.2020.122751>.
18. V. Fierro, V. Torne, Adsorption of phenol onto activated carbons having different textural and surface properties, 111 (2008) 276–284. <https://doi.org/10.1016/j.micromeso.2007.08.002>.
19. D. Zhang, P. Huo, W. Liu, Behavior of phenol adsorption on thermal modified activated carbon, *Chinese J. Chem. Eng.* 24 (2016) 446–452. <https://doi.org/10.1016/j.cjche.2015.11.022>.
20. A. Dehbi, Y. Dehmani, H. Omari, A. Lammini, K. Elazhari, S. Abouarnadasse, A. Abdallaoui, Comparative study of malachite green and phenol adsorption on synthetic hematite iron oxide nanoparticles (α -Fe₂O₃), *Surfaces and Interfaces.* 21 (2020) 100637. <https://doi.org/10.1016/j.surfin.2020.100637>.
21. L. Lupa, L. Cocheci, R. Pode, I. Hulka, Phenol adsorption using Aliquat 336 functionalized Zn-Al layered double hydroxide, *Sep. Purif. Technol.* 196 (2018) 82–95. <https://doi.org/10.1016/j.seppur.2017.10.003>.
22. S. Lv, C. Li, J. Mi, H. Meng, A functional activated carbon for efficient adsorption of phenol derived from pyrolysis of rice husk, KOH-activation and EDTA-4Na-modification, *Appl. Surf. Sci.* 510 (2020) 145425. <https://doi.org/10.1016/j.apsusc.2020.145425>.
23. Y. Dehmani, O. El, H. Mezougane, Comparative study on adsorption of cationic dyes and phenol by natural clays, *Chem. Data Collect.* 33 (2021) 100674. <https://doi.org/10.1016/j.cdc.2021.100674>.
24. A. Supong, P.C. Bhomick, R. Karmaker, S.L. Ezung, L. Jamir, U.B. Sinha, D. Sinha, Experimental and theoretical insight into the adsorption of phenol and 2,4-dinitrophenol onto Tithonia diversifolia activated carbon, *Appl. Surf. Sci.* 529 (2020) 147046. <https://doi.org/10.1016/j.apsusc.2020.147046>.
25. J. Sun, X. Liu, F. Zhang, J. Zhou, J. Wu, A. Alsaedi, T. Hayat, J. Li, Insight into the mechanism of adsorption of phenol and resorcinol on activated carbons with different oxidation degrees, *Colloids Surfaces A Physicochem. Eng. Asp.* 563 (2019) 22–30. <https://doi.org/10.1016/j.colsurfa.2018.11.042>.
26. X. Yan, Y. Li, X. Hu, R. Feng, M. Zhou, D. Han, Enhanced adsorption of phenol from aqueous solution by carbonized trace ZIF-8-decorated activated carbon pellets, *Chinese J. Chem. Eng.* (2020) 2–8. <https://doi.org/10.1016/j.cjche.2020.06.027>.
27. J.P. Castro, A. Napoli, P.F. Trugilho, G.H.D. Tonoli, D.F. Wood, M.L. Bianchi, Pretreatment Affects Activated Carbon from Piassava and, *MDPI.* (2020) 1–13.
28. W. Xiong, W. Cui, R. Li, C. Feng, Y. Liu, N. Ma, J. Deng, L. Xing, Y. Gao, N. Chen, Environmental Science and Ecotechnology Mineralization of phenol by ozone combined with activated carbon: Performance and mechanism under different pH levels, *Environ. Sci. Ecotechnology.* 1 (2020) 100005. <https://doi.org/10.1016/j.ese.2019.100005>.
29. U. Beker, B. Ganbold, H. Dertli, D.D. Gülbayir, Adsorption of phenol by activated carbon: Influence of activation methods and solution pH, *Energy Convers. Manag.* 51 (2010) 235–240. <https://doi.org/10.1016/j.enconman.2009.08.035>.
30. C.K. Balogoun, I. Tchakala, M. Medokponou, M.L. Bawa, D.C. Sohounhloue, Influence of Pretreatment with Soda (NaOH) on the Structural Characteristics of Activated Carbon Prepared by Chemical Means with H₃PO₄ from Rice Bran., *Am. J. Phys. Chem.* 5 (2016) 35. <https://doi.org/10.11648/j.ajpc.20160502.13>.
31. S. Altenor, B. Carene, E. Emmanuel, J. Lambert, J.J. Ehrhardt, S. Gaspard, Adsorption studies of methylene blue and phenol onto vetiver roots activated carbon prepared by chemical activation, *J. Hazard. Mater.* 165 (2009) 1029–1039. <https://doi.org/10.1016/j.jhazmat.2008.10.133>.

32. S.F. Lütke, A. V. Igansi, L. Pegoraro, G.L. Dotto, L.A.A. Pinto, T.R.S. Cadaval, Preparation of activated carbon from black wattle bark waste and its application for phenol adsorption, *J. Environ. Chem. Eng.* 7 (2019) 103396. <https://doi.org/10.1016/j.jece.2019.103396>.
33. Q. Miao, Y. Tang, J. Xu, X. Liu, L. Xiao, Q. Chen, Activated carbon prepared from soybean straw for phenol adsorption, *J. Taiwan Inst. Chem. Eng.* 44 (2013) 458–465. <https://doi.org/10.1016/j.jtice.2012.12.006>.
34. Y. Gokce, S. Yaglikci, E. Yagmur, A. Banford, Z. Aktas, Adsorption behaviour of high performance activated carbon from demineralised low rank coal (Rawdon) for methylene blue and phenol, *J. Environ. Chem. Eng.* 9 (2021) 104819. <https://doi.org/10.1016/j.jece.2020.104819>.
35. G. Lü, J. Hao, L. Liu, H. Ma, Q. Fang, L. Wu, M. Wei, Y. Zhang, The adsorption of phenol by lignite activated carbon, *Chinese J. Chem. Eng.* 19 (2011) 380–385. [https://doi.org/10.1016/S1004-9541\(09\)60224-X](https://doi.org/10.1016/S1004-9541(09)60224-X).
36. A. Mandal, N. Bar, S.K. Das, Phenol removal from wastewater using low-cost natural bioadsorbent neem (*Azadirachta indica*) leaves: Adsorption study and MLR modeling, *Sustain. Chem. Pharm.* 17 (2020) 100308. <https://doi.org/10.1016/j.scp.2020.100308>.
37. B. Xie, J. Qin, S. Wang, X. Li, H. Sun, W. Chen, Adsorption of Phenol on Commercial Activated Carbons: Modelling and Interpretation, *Int. J. Environ. Res. Public Health.* 17 (2020). <https://doi.org/10.3390/ijerph17030789>.
38. H. Jalilvand, F. Feyzi, M.R. Dehghani, Adsorption of dimethyl sulfide from model fuel on raw and modified activated carbon from walnut and pistachio shell origins : Kinetic and thermodynamic study, *Colloids Surfaces A.* 593 (2020) 124620. <https://doi.org/10.1016/j.colsurfa.2020.124620>.